Charge transfer in F^{2+} ions colliding with He atoms below keV energies and its reverse process

J. P. Gu,[1,2] G. Hirsch,[1,*] R. J. Buenker,[1,2] and M. Kimura[1,3]
[1]*Theoretische Chemie, Bergische Universitaet-Gesamthochschule Wuppertal, D-42097 Wuppertal, Germany*
[2]*Harvard-Smithsonian Center for Astrophysics, Cambridge, Massachusetts 02138*
[3]*Graduate School of Science and Engineering, Yamaguchi University Ube, Yamaguchi 755-8611, Japan*

C. M. Dutta and P. Nordlander
Department of Physics and Rice Quantum Institute, Rice University, Houston, Texas 77251-1892
(Received 2 March 2000; published 19 October 2000)

Charge transfer processes in collisions of F^{2+} ions with He atoms were studied by using the molecular representation below 600 eV energies. The ground $F^{2+}(^4S)$ state and one excited $F^{2+}(^2D)$ state are considered as the initial channels in order to examine the effect of the excited state. We have also investigated charge transfer processes in the reverse ion-ion collisions. Cross sections for nonradiative charge transfer in the ground quartet state F^{2+}+He collisions are found to increase gradually with the impact energy and reach around $2\times10^{-16}\,cm^2$ at 558 eV, while those from the doublet state also show a gradual increase and stay nearly constant with $1.2\times10^{-16}\,cm^2$ at the same energy. Cross sections for the reverse processes for both symmetries are found to be very small with a magnitude less than $10^{-18}\,cm^2$ due to the strong Coulomb repulsion between two ions, but rapidly increase as the collision energy increases to reach 3×10^{-17} and $10^{-17}\,cm^2$ for the quartet and doublet manifolds, respectively, at the highest energy studied.

PACS number(s): 34.50.−s, 34.20.Mq

I. INTRODUCTION

Charge transfer processes for heavy-ion impact are important basic processes in various scientific and technological applications [1]. Over the past decade, an intense effort from the atomic physics community toward a better understanding of scattering dynamics over a wide range of energies has resulted in a basic understanding of compiled experimental cross-section data. As a consequence, a large number of extremely interesting new physics has emerged making the field prosperous and lively. However, although there have been a large number of studies of collisions of H^+, $He^{q+},\ldots,O^{q+}$ ions with simple atoms and molecules, relatively few investigations have been performed on other heavy ions ($Z>9$) because of, in part, some difficulties in producing these ions in experiments [2]. However, scattering processes by these ions are particularly interesting and important because not much spectroscopic information for the ions is available, and these complex systems possibly lead us to a new phenomenon of collision physics.

Recently, HF molecules have been detected in interstellar medium, and the origin and formation mechanisms are sought [3]. From this observation, therefore, F^{q+} ions are expected to be present in interstellar environment, and to play a subtle role for astrochemistry. Also, fluorine ions (F^{q+}) and atoms are known to be present in biological systems including the human body, and the knowledge of its interaction with other atoms and molecules are needed for medical and biological study. In a previous publication in our series of investigations of electron capture processes by heavier-ion impact, we have reported the study on Si, S, and P ions [4–6] on H and He atoms. As a part of this project, we here present a theoretical investigation on charge transfer in collision of F^{q+} ions with He atoms based on a molecular state expansion method below 1 keV/u. The processes we are concerned with are (i) the ground-state ion impact

$$F^{2+}(^4S)+He(^1S)\rightarrow F^{+}+He^{+} \tag{1a}$$

and (ii) the excited-state ion impact

$$F^{2+}(^2D)+He(^1S)\rightarrow F^{+}+He^{+}, \tag{1b}$$

and their reverse processes,

$$F^{+}+He^{+}(1s)\rightarrow F^{2+}(^4S)+He(^1S) \tag{1c}$$

and

$$F^{+}+He^{+}(1s)\rightarrow F^{2+}(^2D)+He(^1S). \tag{1d}$$

The energy defect between the ground $F^{2+}(^4S)$ and the excited $F^{2+}(^2D)$ states is approximately 4.3 eV. Therefore, these two ions may be produced simultaneously through γ-ray or ion-impact ionization in the natural environment like the astrophysical environment, or laboratory plasma. Hence, it is necessary to put together all information of the effect from these states when modeling scattering dynamics.

II. THEORETICAL MODEL

A. Molecular states

The adiabatic potential curves of HeF^{2+} are obtained by employing the *ab initio* multireference single- and double-excitation configuration interaction (MRD-CI) method [7], with configuration selection at a threshold of $5.0\times10^{-8}E_h$

*Deceased.

TABLE I. Number of reference configuraions, N_{ref} and number of roots N_{root} treated in each irreducible representation in the present calculation for HeF^{2+} system.

State	N_{ref}/N_{root}
$^2A_1$	75/6
$^2B_1$	36/5
$^2A_2$	33/5
$^4B_1$	20/2
$^4A_2$	39/3

and energy extrapolation, using the Table CI algorithm [8]. The two electrons in the first (lowest) molecular orbital (MO) are kept inactive in the present CI calculation, and the highest MO is discarded. The coupling matrix elements are calculated using the resulting CI wave functions. The radial coupling elements are calculated using a finite-difference method [9]. In the calculation, for the F atom, the *cc-p*VQZ basis set [10] is used, but the *g* function is discarded. In addition to the above basis set, several diffuse functions are added. The basis set for the fluorine atom is thus $(14s8p3d2f)$, contracted to $[7s6p3d2f]$. For the helium atom, the $(10s5p2d)/[7s4p2d]$ basis set is employed. The *s*- and *p*-type functions are from Ref. [11] and two *d*-type functions are from Ref. [12]. The number of reference configurations and the number of roots treated in each irreducible representation in our *ab initio* MRD-CI calculations are listed in Table I. The MO's and their asymptotes thus obtained are shown in Table II.

B. Collision dynamics

A semiclassical MO expansion method with a straight-line trajectory of the incident ion was employed to study the collision dynamics above 50 eV [13]. In this approach, the relative motion of heavy particles is treated classically, while electronic motions are treated quantum mechanically. The total scattering wave function was expanded in terms of products of a molecular electronic state and atomic-type electron translation factors (ETF's), in which the inclusion of the ETF satisfies the correct scattering boundary condition. Note that the atomic ETF may not be correct for adequate description of molecular characters of the colliding system for slow collisions. However, it has been tested extensively and found that reasonable results are obtained. Substituting the total wave function into the time-dependent Schrödinger equation and retaining the ETF correction up to first order in the relative velocity between the collision partners, we obtain a set of first-order coupled equations in time *t*. Transitions between the molecular states are driven by nonadiabatic couplings. By solving the coupled equations numerically, we obtain the scattering amplitudes for transitions: the square of the amplitude gives the transition probability, and integration of the probability over the impact parameter and the azimuthal angle gives the cross section. The molecular states included in the dynamical calculations are the two sets of states, the quartet and doublet states shown in Figs. 1 and 4, respectively.

TABLE II. Asymptotes of FHe^{2+}.

No.	Asymptote	Relative energy Expt. (cm^{-1})	Relative energy Calc. (cm^{-1})	State
1	$F^+(^3P_g)/He^+(^2S_g)$ $(2s^2,2p^4)$	0	50	$(1)^2\Sigma^+,(1)^2\Pi$ $(1)^4\Sigma^-,(1)^4\Pi$
2	$F^+(^1D_g)/He^+(^2S_g)$ $(2s^2,2p^4)$	20 873	21 043	$(1)^2\Sigma^+,(2)^2\Pi$ $(1)^2\Delta$
3	$F^+(^1S_g)/He^+(^2S_g)$ $(2s^2,2p^4)$	44 919	45 189	$(2)^2\Sigma^+$,
4	$F^{2+}(^4S_u)/He(^1S_g)$ $(2s^2,2p^3)$	83 885	81 477	$(2)^4\Sigma^-$
5	$F^{2+}(^2D_u)/He(^1S_g)$ $(2s^2,2p^3)$	117 969	116 289	$(2)^2\Sigma^-,(3)^2\Pi$ $(2)^2\Delta$
6	$F^{2+}(^2P_u)/He(^1S_g)$ $(2s^2,2p^3)$	135 443	134 011	$(3)^2\Sigma^+,(4)^2\Pi$
7	$F^+(^3P_u)He^+(^2S_g)$ $(2s^2,2p^5)$	164 798		$(4)^2\Sigma^+,(5)^2\Pi$ $(1)^4\Sigma^+,(2)^4\Pi$

(i) Quartet states charge-transfer channels $[F^+(^3P_g)+He^+(^2S_g)]$ are $1\,^4\Sigma^-$ and $1^4\Pi$, and the initial channel $[F^{2+}(^4S_u)+He(^1S_g)]$ is $2\,^4\Sigma^-$. For charge-transfer cross-section calculations of the quartet states, we included $(1\,^4\Sigma^-,1\,^4\Pi)$ and $2\,^4\Sigma^-$ (see Table II). The MO's in the same parentheses are degenerate states. The next higher states are $(1\,^4\Sigma^+,2\,^4\Pi)$ with an energy 80 913 cm^{-1} higher.

(ii) Doublet states: charge transfer channels $[F^+(^3P_g)+He^+(^2S_g)]$ are $1\,^2\Sigma^-$ and $1\,^2\Pi$, and charge-transfer–excitation channels $[F^+(^1D_g)+He^+(^2S_g)]$ are $1\,^2\Sigma^+$, $2\,^2\Pi$, and $1\,^2\Delta$; charge transfer excitation channel $[F^+(^1S_g)+He^+(^2S_g)]$ is $2\,^2\Sigma^+$. The initial channels $[F^{2+}(^2D_u)+He(^1S_g)]$ are $2\,^2\Sigma^-$, $3\,^2\Pi$, and $2\,^2\Delta$. We coupled eleven states, $(1\,^2\Sigma^-,1\,^2\Pi)$, $(1\,^2\Sigma^+,2\,^2\Pi$, $1\,^2\Delta(^1A_1,^2A_1))$, and $(2\,^2\Sigma^+,2\,^2\Sigma^-,3\,^2\Pi$, and $2\,^2\Delta(^1A_1,$ $^2A_1))$. (see Table II).

III. RESULTS AND DISCUSSIONS

In the following sections, we discuss the quartet and doublet states separately.

A. Adiabatic potentials and corresponding couplings

1. Quartet states

Figure 1 shows the potential energies for the three quartet states for separations *R* up to $20a_0$. Because the colliding particles have an electron structure that is tightly bound, we can expect that two particles do not begin to interact until they come closer to sufficiently small *R*, and further, they have only the weak interaction. Consequently, a weak avoided crossing is seen between $1\,^4\Sigma^-$ and $2\,^4\Sigma^-$ at $R \sim 3.7a_0$. Apart from this avoided crossing, no other mixing of states can be found among the present states. As expected, the corresponding radial coupling matrix element between $1\,^4\Sigma^-$ and $2\,^4\Sigma^-$ shown in Fig. 2 peaks near this avoided crossing. The rotational coupling matrix elements are shown

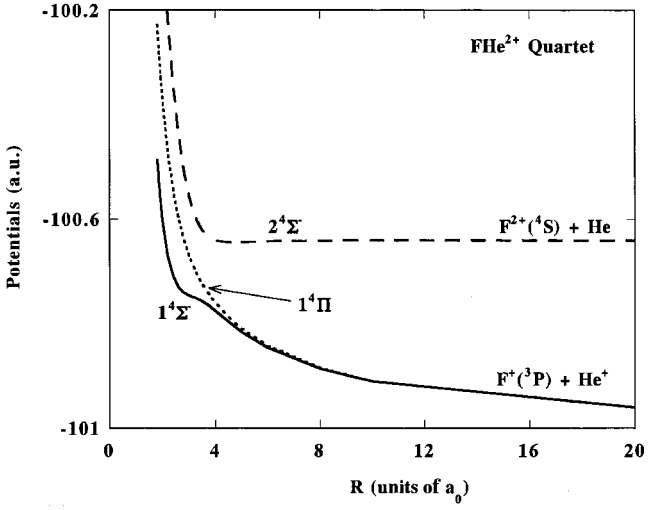

FIG. 1. The adiabatic potentials for the quartet states of the FHe^{2+}.

in Fig. 3. The matrix element between $2\,^4\Sigma^-$ and $1\,^4\Pi$ peaks at $R\sim 2.5a_0$ and becomes negligible at R beyond $\sim 7a_0$. The $1\,^4\Pi$ and $1\,^4\Sigma$ states are degenerate, and therefore, the rotational coupling matrix element approaches a finite constant value at large R. Note that in Fig. 3, these rotational coupling matrix elements shown are not multiplied by b^2/R^2 where b represents the impact parameter. However, the long-range coupling is suppressed by the introduction of the ETF. Overall, the reaction occurs in the region of R less than $5a_0$.

2. Doublet states

Figure 4 displays the potentials where the dotted lines are for the Σ states, chains for the Π states, and broken lines with diamonds are for the Δ states, respectively. There is no obvious strong mixing of molecular states, similar to the situation for the quartet manifold described above. Consequently, beyond $\sim 5a_0$, it appears that all states recover their respective atomic character, and therefore, no strong coupling among these states is observed. Figures 5(a) and 5(b) illustrate the representative radial coupling matrix elements, and Figs. 6(a)–6(d) for the rotational coupling matrix elements.

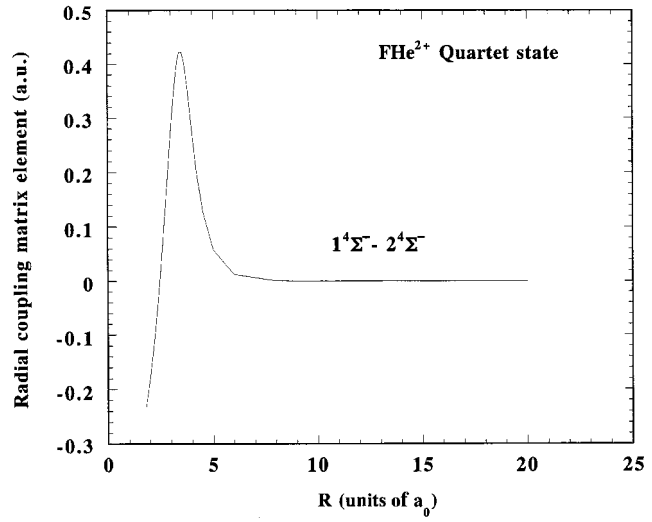

FIG. 2. The radial coupling matrix elements of the quartet states.

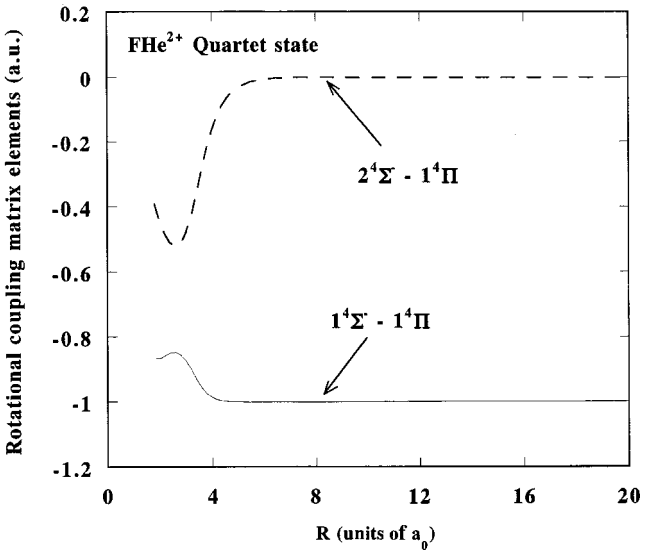

FIG. 3. The rotational coupling matrix elements of the quartet states.

Note that double capture channels lie much higher with the approximate energy defect of 26.6 eV that is not easily accessible in the present collision energy, and hence, in the present calculation, we ignored these double capture channels.

B. Charge transfer cross sections

1. Quartet states

a. $F^{2+}+He(^1S)$ *collisions.* As seen from Table II, the incoming channel is $2\,^4\Sigma^-$, and the single charge trans-

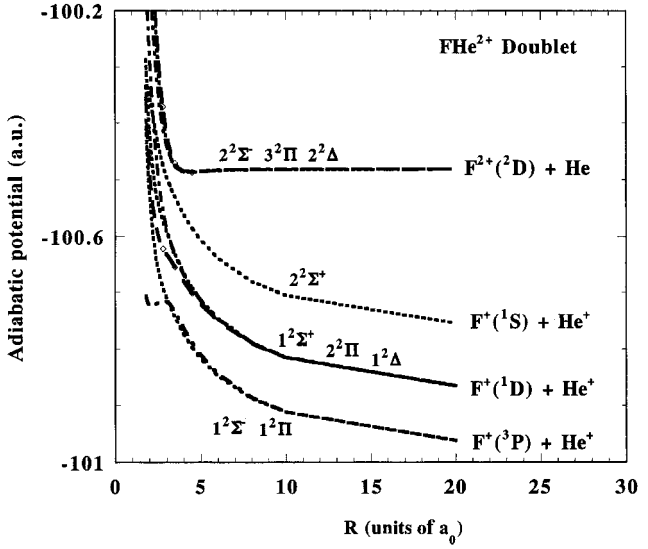

FIG. 4. The adiabatic potentials for the doublet states of the FHe^{2+}.

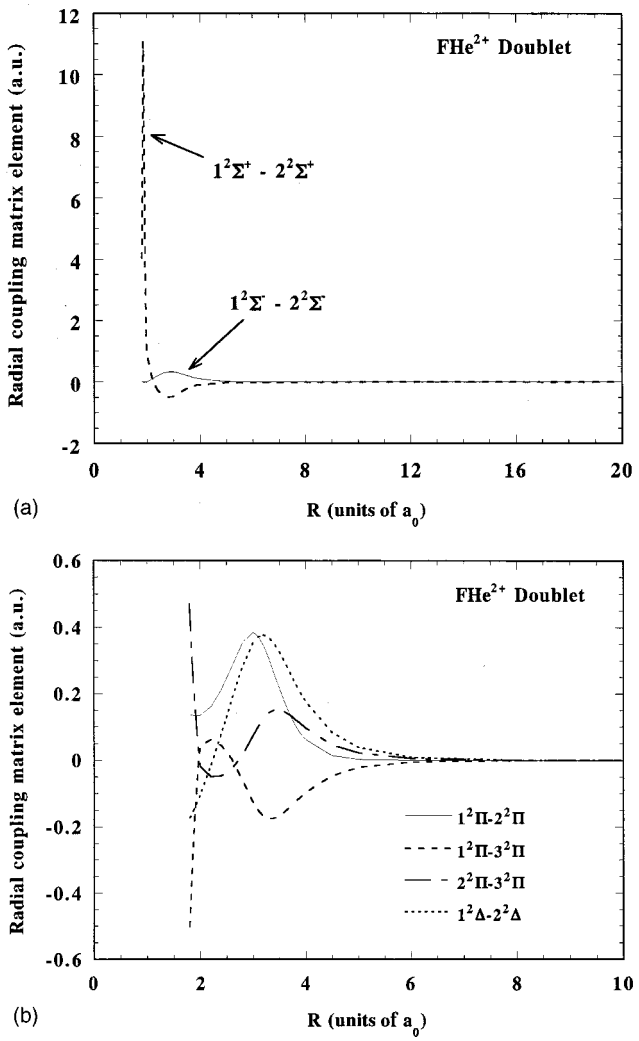

FIG. 5. The representative radial coupling matrix elements for the doublet states.

ferred states are $1\ ^4\Sigma^-$, and $1\ ^4\Pi$. This is an exthothermic process. The partial cross sections for $1\ ^4\Sigma^-$, and $1\ ^4\Pi$ channels and the sum of these (total cross section) are included in Fig. 7. The cross sections increase fourfold as the incident energy increases from 0.1 to 0.6 keV/u, but are found to be rather small with a magnitude of $2\times10^{-16}\,\mathrm{cm}^2$ even at the highest energy studied. This is a manifestation of the weak coupling that connects between the initial and charge transferred states because both the projectile F^{2+} and the target He atom have tight shells. The partial cross sections for $1\ ^4\Sigma^-$ are larger than those for $1\ ^4\Pi$, and they show a structure at collision energies between 0.2–0.3 keV. This is an effect of interference between the initial $2\ ^4\Sigma^-$ and $1\ ^4\Sigma^-$ states. The $1\ ^4\Pi$ state is not involved in the dynamics. The total cross sections reflect this structure. This is caused by the strong peak in the coupling of this $1\ ^4\Sigma^-$ channel with the incoming channel at $R\sim3.7a_0$ (see Fig. 2). The partial cross sections for $1\ ^4\Pi$ increase with the collision energy monotonously.

$F^+ + He^+$ collisions. The incoming channels are two degenerate states, $1\ ^4\Sigma^-$ and $1\ ^4\Pi$, and the outgoing channel is $2\ ^4\Sigma^-$. Figure 8 shows the calculated cross sections for each incoming channel and the cross sections averaged over the two incoming channels. In this case also, because of the strong coupling between $1\ ^4\Sigma^-$ and $2\ ^4\Sigma^-$ states, the cross sections are larger when the incoming channel is $1\ ^4\Sigma^-$ state, and we observe a similar structure at a collision energy ~0.25 keV/u. The cross sections are about 30% of those for the reverse $F^{2+}+\mathrm{He}(^1S)$ collision with a magnitude of $0.6\times10^{-16}\,\mathrm{cm}^2$ at the highest energy. This is because this reaction is an endothermic process, and moreover, because the two positive charges prohibit the two particles to come sufficiently close for strong interaction.

2. Doublet states

a. $F^{2+}+He(^1S)$ collisions. The $2\ ^2\Sigma^-$, $3\ ^2\Pi$, and $2\ ^2\Delta(^2A_1, ^2A_2)$ states correspond to the incoming $[\mathrm{F}^{2+}+\mathrm{He}(^1S)]$ channels. The partial cross sections of single charge transfer corresponding to each of the incoming channels are shown in Fig. 9. The cross sections for the $2\ ^2\Delta(^2A_2)$ incoming channel are the same as those for $2\ ^2\Delta(^2A_1)$ and hence, are treated accordingly. In the calculation, we included the rotational coupling matrices for which $\Delta\Lambda=\pm1$. For the rotational coupling between Π and Δ states, only those matrix elements for Δ and Π that are degenerate are included. Figures 9(a)–9(e) show the partial cross sections for each of these incoming channels. When the incoming channel is the $2\ ^2\Sigma^-$ state [Fig. 9(a)], the $1\ ^2\Sigma^-$ partial cross sections show a weak but non-negligible structure at the lower collision energies below 0.3 keV/u. This structure is caused by the small peak near $R=3a_0$ in the radial coupling matrix element between $2\ ^2\Sigma^-$ and $1\ ^2\Sigma^-$ states, seen in Fig. 5(a). Also, the $1\ ^2\Sigma^-$ and $1\ ^2\Pi$ partial cross sections increase with the collision energy, but the other partial cross sections remain almost constant. When the $3\ ^2\Pi$ state is the incoming channel [Fig. 9(b)], we do not observe the structure seen in the $1\ ^2\Sigma^-$ partial cross sections, hence indicating a weak rotational coupling. Here also, the $1\ ^2\Pi$ and $1\ ^2\Sigma^-$ partial cross sections increases with the collision energy, but the other partial cross sections remain almost constant. When the $2\ ^2\Delta(^1A_1)$ or $2\ ^2\Delta(^2A_1)$ state [see Fig. 9(c)] is the incoming channel, the $2\ ^2\Sigma^+$ partial cross sections stay nearly constant in the entire energy range and other partial cross sections only slowly increase with the collision energy. When the incoming channel is $3\ ^2\Pi$, the cross sections are more than a factor of 2 larger than for the incoming channel of $2\ ^2\Sigma^-$. In Fig. 10, we compare total cross sections from each incoming channel. We see that the cross sections for $3\ ^2\Pi$ and the sum of cross sections for $2\ ^2\Delta(^1A1)$ and $2\ ^2\Delta(^2A2)$ are comparable, and about 2.5 times larger than those for the $2\ ^2\Sigma^-$ incoming channel. The average cross sections, obtained by summing the total cross sections from the four incoming channels and dividing by 4, are also shown in the same figure. A value of the total cross section reaches approximately $1\times10^{-16}\,\mathrm{cm}^2$ at 0.6 keV/u.

b. $F^+ + He^+$ collisions. The incoming channels are the

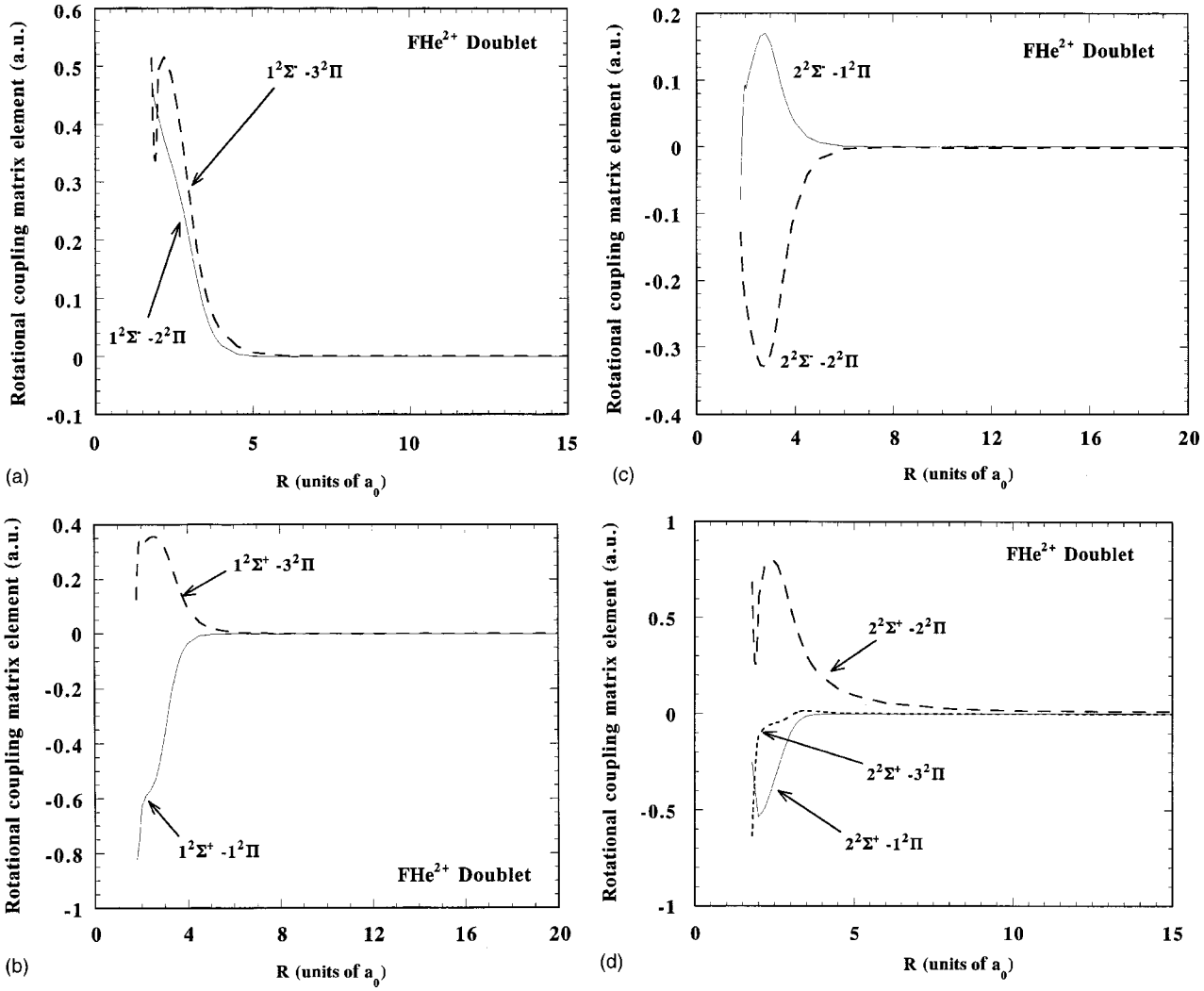

FIG. 6. The representative rotational coupling matrix elements for the doublet states.

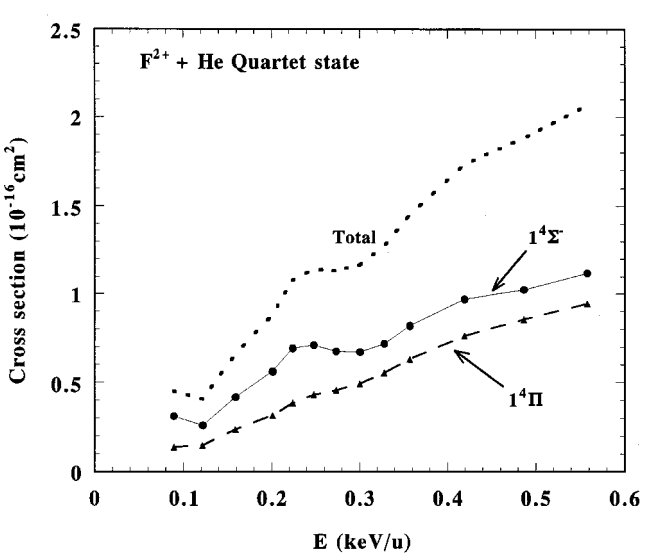

FIG. 7. Partial and total charge transfer cross sections for process (a); $F^{2+}+He \rightarrow F^{-}+He^{+}$ in the quartet state.

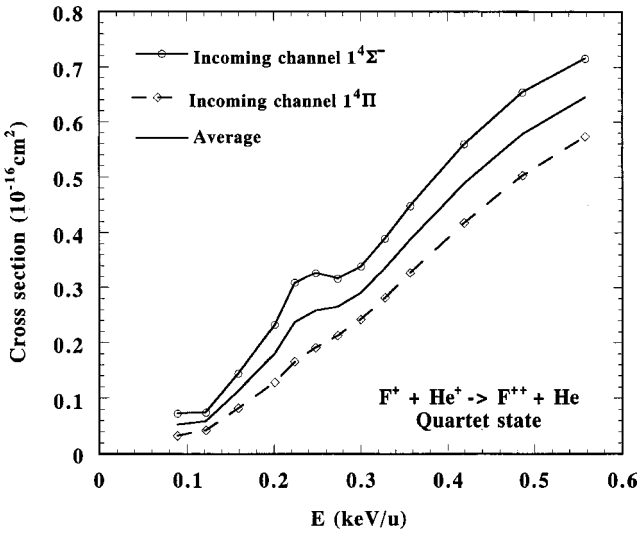

FIG. 8. Charge transfer cross sections for different initial incoming channels and the average in process (b); $F^{+}+He^{+}(F^{2+}+He)$ in the quartet state.

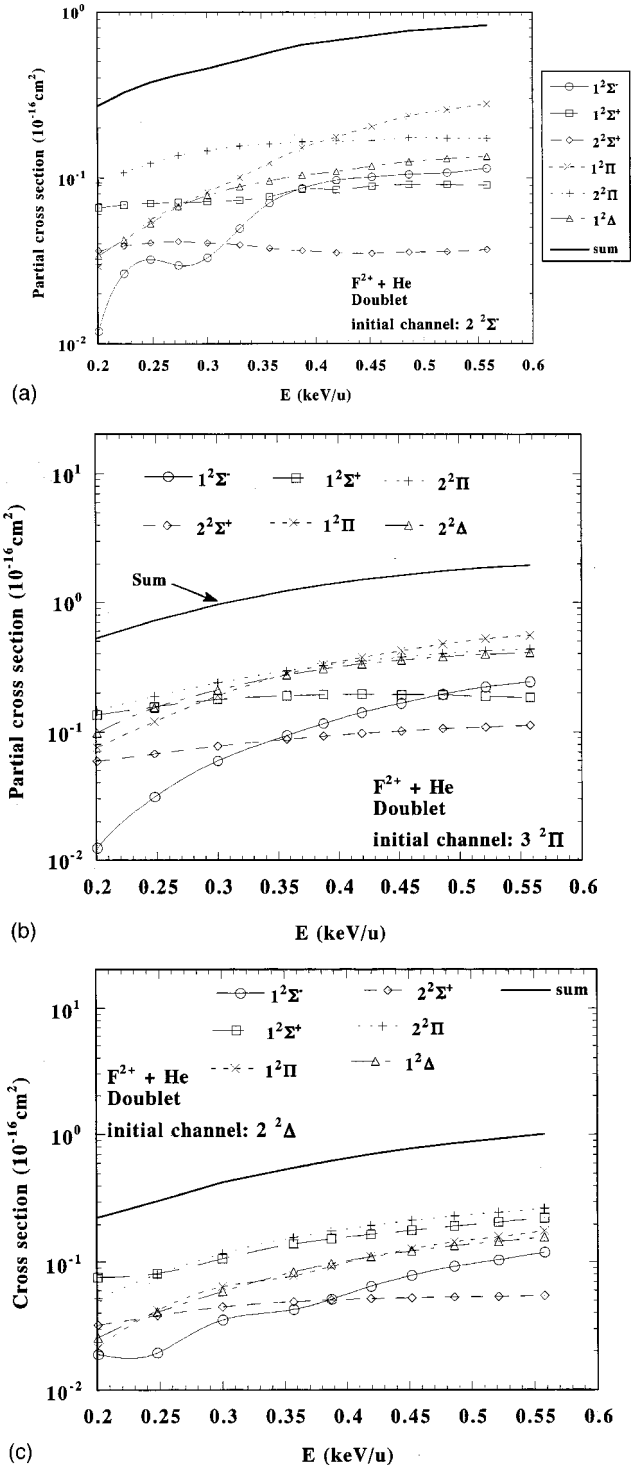

FIG. 9. (a) Partial charge transfer cross sections for process (a); $F^{2+}+He(F^{2+}He^{+})$ in the doublet state when the incoming channel is $2\ ^2\Sigma^-$. (b) The same as in (a) except that the incoming channel is $3\ ^2\Pi$. (c) The same as in (a) except that the incoming channel is $2\ ^2\Delta$.

ground states for the $F^{+}+He^{+}$ system, namely, $1\ ^2\Sigma^-$ and $1\ ^2\Pi$ states. Figure 11 shows the partial cross sections for these two incoming states; they do not show any structure. The $2\ ^2\Pi$ partial cross sections dominate.

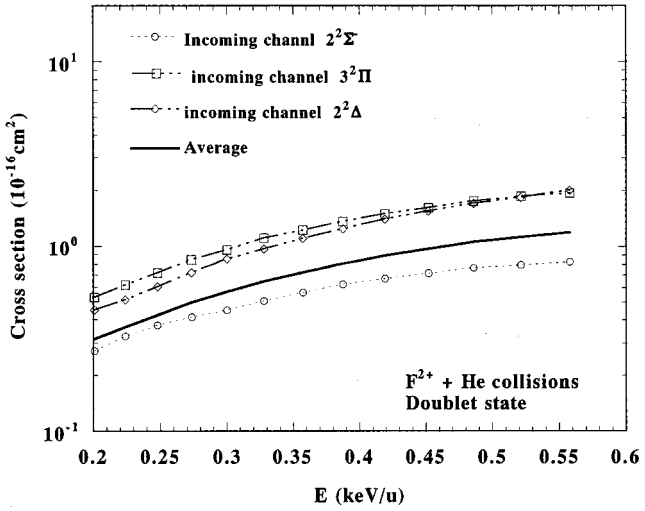

FIG. 10. Charge transfer cross sections for different incoming channels, and the average over the incoming channels for process (a); $F^{2+}+He\rightarrow F^{+}+He^{+}$ in the doublet state.

IV. CONCLUSIONS

Charge transfer processes in collision of F^{2+} ions with He atoms and its reverse processes have been investigated theoretically using the molecular representation below 0.6 keV/u. The quartet (the ground state) and doublet (first excited state) states for the initial channel are considered for $F^{2+}+He$ collisions. The magnitude of the cross sections for charge transfer by the ground-state $F^{2+}(^4S)$ ion impact is nearly the same as those by the excited state $F^{2+}(^2D)$ ion impact. The ion-ion collision both for the quartet and doublet manifolds is found to be less effective in the entire collision energies and corresponding cross sections are smaller by one to two orders of magnitude. This effect is due in part to the strong repulsion between two positively charged ions.

ACKNOWLEDGMENTS

This work was supported in part by the Grant-in-Aid, the Ministry of Education, Science and Culture, Japan through

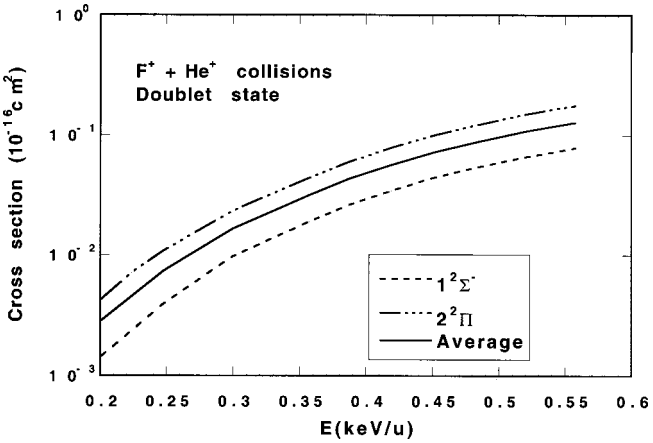

FIG. 11. Partial charge transfer cross sections and sum for process (b); $F^{+}+He^{+}\rightarrow F^{2+}+He$ in the doublet state.

Yamaguchi University and in collaboration with Dr. T. Kato at National Institute for Fusion Science (M.K.); by Deutsche Forschungsgemeinschaft in the form of a Forschergruppe and Grant No. Bu450/7; by the National Science Foundation through a grant to the Institute for Theoretical Atomic and Molecular Physics at Harvard University and Smithsonian Astrophysical Observatory (M.K., J.P.G., and R.J.E.); by NSF/INT9911858; and the Robert A. Welch Foundation (P.N., C.M.D.). The financial support of the Fonds der Chemischen Industrie is also gratefully acknowledged.

[1] R. K. Janev, *Review of Fundamental Processes and Applications of Atoms and Ions* (World Scientific, Singapore, 1993).

[2] R. K. Janev, *Atomic and Molecular Processes in Fusion Edge Plasma* (Plenum, New York, 1995).

[3] D. A. Neufeld, J. Zmuidzinas, P. Schilke and T. G. Phillips, Astrophys. J. Lett. **488**, L141 (1997).

[4] S. Suzuki, N. Shimakura, J.-P. Gu, G. Hirsch, R. J. Buenker, M. Kimura, and P. C. Stancil, Phys. Rev. A **60**, 4504 (1999).

[5] J.-P. Gu, G. Hirsch, R. J. Buenker, M. Kimura, C. M. Dutta, and P. Nordlander, Phys. Rev. A **59**, 405 (1999).

[6] M. Kimura, J.-P. Gu, G. Hirsch, R. J. Buenker, A. Domondon, T. Watanabe, and H. Sato, Phys. Rev. A **56**, 1892 (1997).

[7] R. J. Buenker and S. D. Peyerimhoff, Theor. Chim. Acta **35**, 33 (1974); *ibid.* **39**, 217 (1975); R. J. Buenker, Int. J. Quantum Chem. **29**, 435 (1986). S. Krebs and R. J. Buenker, J. Chem. Phys. **103**, 5613 (1995).

[8] R. J. Buenker, in *Proceedings of the Workshop on Quantum Chemistry and Molecular Physics, Wollongong, Australia*, edited by P. G. Burton (University Press, Wollongong, 1980); in *Studies in Physical and Theoretical Chemistry*, edited by R. Carbo, Current Aspects of Quantum Chemistry Vol. 21 (Elsevier, Amsterdam, 1981), p. 17; R. J. Buenker and R. A. Phillips, J. Mol. Struct.: THEOCHEM **123**, 291 (1985).

[9] G. Hirsch, P. J. Bruna, R. J. Buenker, and S. D. Peyerimhoff, Chem. Phys. **45**, 335 (1980).

[10] T. H. Dunning, Jr., J. Chem. Phys. **90**, 1007 (1989).

[11] K. K. Sunil, J. Lin, H. Siddiqui, P. E. Siska, K. D. Jordan, and R. Shepard, J. Chem. Phys. **78**, 6190 (1983).

[12] D. E. Woon and T. H. Dunning, Jr., J. Chem. Phys. **100**, 2975 (1994).

[13] M. Kimura and N. F. Lane, in *Advances in Atomic, Molecular and Optical Physics*, edited by D. R. Bates and B. Bederson (Academic, New York, 1989), Vol. 26, p. 79.